Journal of New Materials for Electrochemical Systems 13, 227-233 (2010)

Electrochemical Characterization of IrO_2-Pt and RuO_2-Pt Mixtures as Bifunctional Electrodes for Unitized Regenerative Fuel Cells

I.L. Escalante-García[1], S.M. Duron-Torres[1,*] J.C. Cruz[2] and L.G. Arriaga-Hurtado[2]

[1]UACQ-UAZ, CU Siglo XXI-Edificio 6, Km. 6 Carr. Zac.-Gdl., La Escondida, Zacatecas, Zac. C.P. 98160, México
[2]CIDETEQ S.C., Parque Tecnológico Querétaro, Sanfandila, Pedro Escobedo, Qro. C.P. 76703, México

Received: November 19, 2009, Accepted: January 29, 2010

Abstract: *Unitized Regenerative fuel Cell (URFC) is an attractive and efficient method for producing hydrogen and clean energy. Nevertheless, to combine a polymer electrolyte water electrolyzer (PEMWE) and a polymer electrolyte fuel cell (PEMFC) is still a big challenge. Here, it is necessary to overcome several practical and structural features. For instance, the oxygen reduction (ORR) and the water oxidation (OER) are the limiting reaction steps at the oxygen electrode for PEMFC or PEMWE, respectively. Therefore, its high-efficiency depends on the type of electrocatalysts and the capability of the oxygen electrode to operate under the PEMFC or PEMWE conditions. As a consequence, a broad research is focused on developing a new design for the oxygen electrode in URFCs. In this work, several bifunctional electrodes for OER and ORR were designed by mixing electrocatalysts of Pt and IrO_2 or Pt and RuO_2 supported on Ebonex®. Electrochemical characterization by CV, LV and EIS in aqueous 0.5 M H_2SO_4 reveals that IrO_2-Pt and RuO_2-Pt supported on Ebonex®, exhibit high electrocatalytic properties for ORR and OER showing up a possible use in URFCs. In addition, IrO_2 based electrodes display a higher stability than those based on RuO_2.*

Keywords: URFC, IrO_2, RuO_2, bifunctional electrodes.

1. INTRODUCTION

Hydrogen obtained from renewable energy resources is a virtually unlimited, environmentally benign energy source that could meet most of our future energy needs [1,2]. This methodology is an idealized energy cycle. For instance, electricity from renewable energy sources is used to electrochemically split water into hydrogen and oxygen. The only input to this cycle is the clean renewable energy and the only output is electric power, specifically, hydrogen as energy carrier [3]. In this way, a unitized regenerative fuel cell (URFC) is a promising single electrochemical cell that meets the required features of an idealized energy cycle. A URFC is a system which can operate as polymer electrolyte water electrolyzer (PEMWE) or as polymer electrolyte fuel cell (PEMFC). In the PEMWE mode, water is converted into hydrogen and oxygen by using electricity from renewable energies such as solar or wind; then, in the PEMFC mode, the stored hydrogen and oxygen are supplied to generate electrical power and water [4,5]. For its characteristics, a URFC can be used not only for space application but also in one-site energy storage system reducing cost, weight, volume and complexity compared with a regenerative fuel cell (RFC) that separates the PEMWE and the PEMFC. Also, URFCs have the advantages of being free from self-discharges and of giving theoretically higher energy densities compared to secondary batteries [6,7].

The performance of the URFC mainly depends on the structure and the electrochemical characteristics of the oxygen electrode. It is well known that the oxygen reactions, oxygen evolution (OER) and oxygen reduction (ORR), are the slowest steps in several electrochemical processes such as water electrolysis (PEMFC) and energy generation (PEMFC) [8,9]. In a URFC system is believed that the OER is the main source of energy loss due to the complexity of its reaction pathway that involves absorbed species on the catalyst surface blocking the surface sites where they are going to be oxidized. In addition, the oxygen electrode should be resistant to anodic corrosion during OER [5,10]. In consequence, the development of efficient bifunctional electrocatalysts for the oxygen electrode is a technological challenge for the URFCs commercialization.

It has been reported that noble metals and metal oxides have

*To whom correspondence should be addressed: Email: duronsm@prodigy.net.mx
Phone: (492) 9256690 Ext. 6130

been used as bifunctional electrocatalysts on the oxygen electrode [6-7,10-12]. Even though platinum is the best catalyst for ORR, it shows a low catalytic activity for OER. Therefore, several studies have shown that noble metal oxides, such as iridium oxide (IrO_2) and ruthenium oxide (RuO_2), exhibiting good performance for OER [10-14]. Mixing an efficient catalyst for ORR and an efficient catalyst for OER, it could result in an easy methodology for preparing bifunctional electrodes [4,14-17]. However, these electrodes may result in a poor combination between Pt and IrO_2 or Pt and RuO_2; as a consequence, a poor electron conduction could be observed, even if the load of noble metals is quite high. Nonetheless, it is recognized that the use of mixed metals can lead to synergetic effects that could improve the kinetics for the oxygen reactions and the stability/selectivity of the oxygen electrode.

In the oxygen electrode design, it is important to consider the use of catalyst supports. It is widely recognized that a catalyst support provides a good electronic conductivity, as well a high-surface area to lead the catalyst dispersion; consequently, a reduction of the catalyst load is achieved. Carbon is the best conductive and generally used support in PEMFC. However, it is electrochemical unstable at high potential at the oxygen electrode in the PEMWE mode [4,18]. For these reasons, some works have been emerged in order to find an alternative support to carbon [10,19-20]. Conductive oxides as suboxides of titanium dioxide, commercially known as Ebonex®, are strong candidates for their use in URFCs. The advantage of using this material is due to their electrochemical and thermal oxidation stability and relatively high-surface area.

In the present work, highly-active bifunctional electrodes were developed by mixing Pt- nanoparticles and iridium oxide (IrO_2) or ruthenium oxide (RuO_2) electrocatalyst for the kinetics of oxygen reduction and oxygen evolution reactions in URFCs. The bifunctional electrodes were also supported on Ebonex® in order to investigate their electrocatalytic properties by reducing the electrocatalyst load. The ratio of Pt, IrO_2 and RuO_2 were varied from 100 wt % to 30 wt %. Electrochemical measurements by cyclic voltammetry, rotating disk electrode and electrochemical impedance spectroscopy showed that the best bifunctional electrocatalyst was the IrO_2-Pt mixture. IrO_2 and RuO_2 were obtained from novel colloidal method at low temperature showing a particle size less than 10 nm [21].

2. EXPERIMENTAL

2.1. Synthesis and characterization of iridum oxide and ruthenium oxide

Iridium oxide and Ruthenium Oxide precursors were synthesized by a novel colloidal methodology. A low-temperature calcination treatment was carried out in order to obtain the iridium and ruthenium oxides [21]. The resulting powders were characterized by X-ray diffraction (XRD) and by transmission electron microscopy (TEM). A Philips X-Pert diffractometer with a radiation source of K_α at the cupper line (K_α Cu) was operated at 40 kV and 20 mA in order to determine the crystallographic structure and particle size. A Philips CM12 instrument was used to evaluate the catalyst microscopic morphology.

2.2. Electrodes preparation

The electrodes for studying the oxygen evolution were prepared from IrO_2 and RuO_2 synthesized powders unsupported and supported on Ebonex® (Atraverda). The OER and ORR were studied on bifunctional electrodes prepared by mixing IrO_2 or RuO_2 with commercial Pt-nanoparticles (fuel cell grade, Strem Chemical). Table 1 shows the weight ratio of electrocatalyst(s):Ebonex® used to prepare each electrode. Each sample was added with an appropriate amount of Nafion® (5%, Aldrich), ethylic alcohol (spectroscopy grade, Aldrich) and triple distilled water. The resulting solutions were placed under ultrasonication for 0.5 h in order to obtain a highly dispersed ink. Subsequently, a specific volume of each ink was casted on a clean glassy carbon disk electrode (GCE) ($A = 0.07\ cm^2$). The coated GCEs were dried in a furnace at 80°C for 10 min.. Finally, IrO_2, RuO_2, IrO_2-Pt or RuO_2-Pt films were used as working electrodes for the OER and ORR kinetic studies. The catalyst load on each GCE was calculated by measuring the catalyst ink density.

2.3. Electrochemical characterization of bifunctional electrodes

Cyclic voltammetry (CV) was carried out to evaluate the effect of the Pt-nanoparticles and the Ebonex® in the IrO_2 or RuO_2 electrodes by scanning the potential at 50 mV s^{-1} between -0.69 V and 0.75 V (vs. Hg/Hg_2SO_4/0.5 M H_2SO_4) under a N_2 –atmosphere electrolyte solution. Oxygen evolution experiments were performed by lineal voltammetry (LV) at a scan rate of 5 mV s^{-1} in the anodic direction from 0.32 V to 1.02 V (vs. Hg/Hg_2SO_4/0.5 M H_2SO_4) in O_2-free electrolyte solution. In addition, electrochemical impedance spectroscopy (EIS) experiments were carried out in the potentiostatic mode in the 100 kHz to 10 mHz frequency range. The impedance spectra were registered with a logarithmic data collection scheme at 10 steps per decade with an amplitude of 10 mV. Rotating-disk electrode (RDE) measurements were done to determine the kinetics of oxygen-reduction in O_2-saturated solution. The potential was scanned in the cathodic direction from the open circuit potential (E_{oc}) to -0.20 V (Hg/Hg_2SO_4/0.5 M H_2SO_4) at 5 mV s^{-1}. The RDE experiments were performed several times at different frequency (*f*), 100 to 1600 rpm.

All the experiments were performed in a double-compartment electrochemical glass cell. A Hg/Hg_2SO_4/0.5 M H_2SO_4 (ESM = 0.68V vs. NHE) electrode was used as reference which was positioned as close to the working electrode as possible by means of a Luggin capillary. A Pt-mesh was used as counter-electrode and the aqueous electrolytic medium was 0.5 M H_2SO_4 at room temperature. The electrochemical measurements were performed using an EG&G PAR system model VersaSTAT 3 Potensiostat/Galvanostat.

Table 1. IrO_2, RuO_2 and Pt ratios used for preparing bifunctional oxygen electrodes.

Electrode	IrO_2	RuO_2	Pt	Ebonex®
	wt %			
1	100	-	-	-
2	-	100	-	-
3	30	-	-	70
4	-	30	-	70
5	-	-	30	70
6	30	-	30	40
7	-	30	30	40

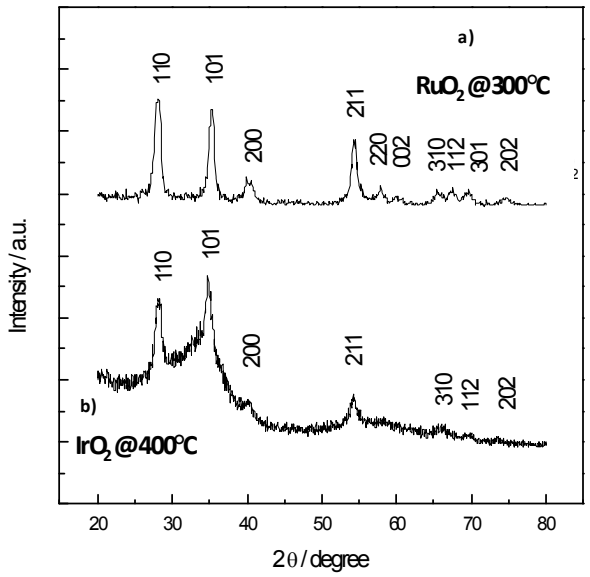

Figure 1. XRD patterns of the metal oxides electrocatalysts. a) RuO_2 calcined at 350° for 1 h; b) IrO_2 calcined at 400°C for 1 h.

The rotation rate was controlled by a PINE MSRX precision rotating system. In this study, all measured values of potential are reported respect to the normal hydrogen electrode (NHE).

3. RESULTS AND DISCUSSION

3.1. Characterization of IrO_2 and RuO_2

Figure 1 shows XRD patterns of the IrO_2 and RuO_2 precursors powders after calcination at 400°C and 300°C for 1 h, respectively. For both metal oxides, all peaks are assigned a rutile crystal structure (110) [5,10,22]. No presence of Ir and Ru in a metallic form is observed. In addition, it is observed that IrO_2 – pattern shows broader peaks than those observed for RuO_2, which implies that RuO_2 crystallize at lower temperatures than IrO_2. The crystallite size of IrO_2 and RuO_2 are about 7 nm and 10.7 nm, respectively, calculated from Scherrer equation [23]. As well, the particle size was studied by TEM (Data not showed). The data reveal that the crystallite size for IrO_2 and RuO_2 are 2.5 nm and 8.6 nm, respectively. The difference observed for IrO_2 particle size is mainly attributed to the formation of not well defined crystals during the powder precursor synthesis. In contrast, the RuO_2 presents a mayor control in its crystal formation.

3.2. Cyclic voltammetry performance

The influence of Ebonex® as electrocatalyst support was studied by CV. Figure 2 displays cyclic voltammograms (CVs) obtained for IrO_2 and RuO_2 unsupported and supported on Ebonex® in N_2 saturated 0.5 M H_2SO_4 solution. The CVs reveal that the electrochemical responses for IrO_2 and RuO_2 change considerably with the use of Ebonex®. For IrO_2 unsupported, two pairs of slightly peaks are localized around 0.3 V (NHE) and 1.0 V (NHE). These peaks are attributed to the redox couple Ir(III)/Ir(IV) and (IV)/Ir(V), respectively [6]. Previous reports suggested that the activity of IrO_2 for the OER is due to the Ir(III)/Ir(IV) redox couple. On the other hand, it is observed that the response for 30 wt % IrO_2 supported on Ebonex® changes dramatically, Figure 2a. First, the two pairs of peaks are not clearly defined. Second, the current density resulting in the anodic up-limit diminishes around a seventy-percent compared with that registered for IrO_2-unsupported. Moreover, the starting potential for the OER changed from 1.4 V(NHE) to 1.45 V(NHE) for IrO_2 supported on Ebonex®. These preliminary results indicate that the inclusion of Ebonex® as support is not at all convenient.

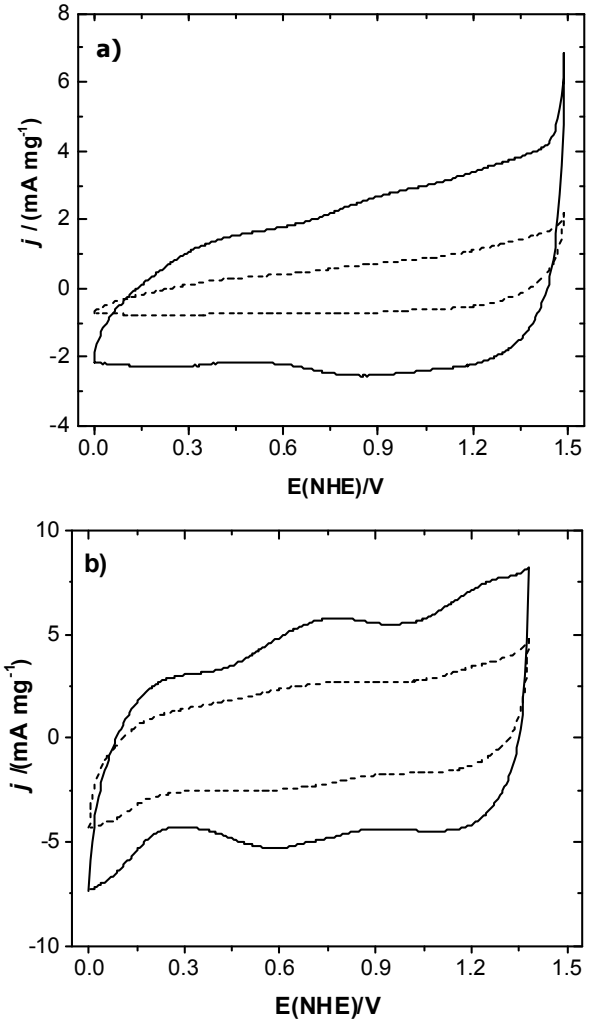

Figure 2. Cyclic voltammograms of GCEs coated with metal oxides and Ebonex® in 0.5 M H_2SO_4 at 50 mV s^{-1}. **a)** IrO_2 (solid line) and 30 wt % IrO_2/Ebonex (dashed line); **b)** RuO_2 (solid line) and RuO_2 and 30 wt% RuO_2/Ebonex (dashed line). Atmosphere: N_2Temperature: Room.

The CVs obtained for RuO_2 unsupported and supported on Ebonex® are similar as shown in Figure 2b. A pair of broad peaks are localized around 0.7 V (NHE) which correspond to the Ru(III)/Ru(IV) redox surface transition [6,24]. For both electrodes, the start potential for OER is quite similar, 1.32 V(NHE) on RuO_2 unsupported and 1.35 V(NHE) on 30 wt % RuO_2/Ebonex®. These

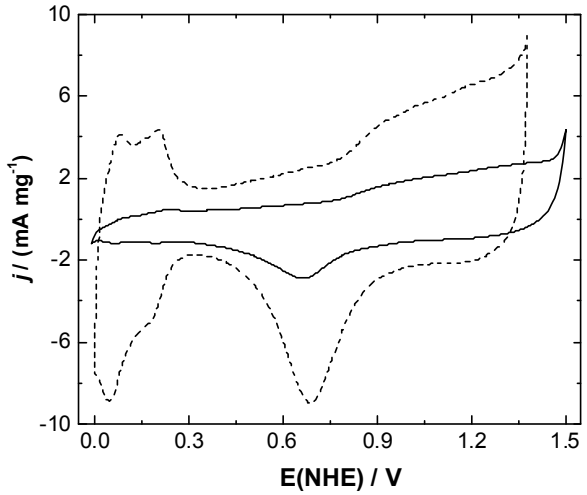

Figure 3. Cyclic voltammograms of GCE electrode coated with (30 wt % RuO_2 – 30% wt Pt) / Ebonex (dashed line) and (30 wt % IrO_2 – 30% wt Pt) / Ebonex (solid line) in 0.5 M H_2SO_4 at 50 mV s^{-1}. Atmosphere: N_2. Temperature: room.

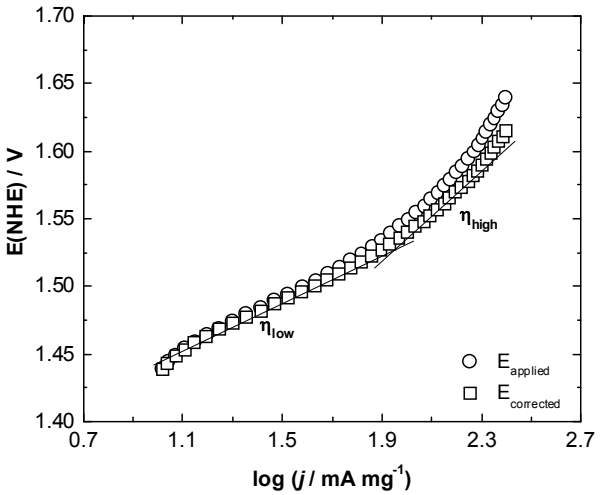

Figure 4. Tafel – Plot for OER on IrO_2 unsupported before (○)and after (□) IR correction.

values are less than those registered for the IrO_2-based electrodes tested and some reported in the literature. [10-11,25]. In addition, the current density is reduced by fifty-percent when the RuO_2 is supported on Ebonex®. It suggests that there is a better dispersion of RuO_2 over the Ebonex® surface in comparison with the IrO_2/Ebonex® electrodes. Finally, the well defined crystalline particles confer more active sites as a result the RuO_2 shows a major selectivity for OER.

The CVs obtained for the mixture IrO_2 – Pt and RuO_2 – Pt supported on Ebonex® are showed in Figure 3. The results clearly reveal the incorporation of Pt to the metal oxides by identifying the hydrogen adsorption region and the adsorbed oxygen region [26]. The current peaks corresponding to hydrogen adsorption /desorption phenomena are localized in the potential range between -0.05 V and 0.30 V. The regions associated to the formation of oxygen-containing species (Pt-O, Pt-OH) start at about 0.75 V for both RuO_2-Pt and IrO_2-Pt Electrodes. The well-defined cathodic peak corresponds to the reduction of the adsorbed oxygen species, 0.70 V. Nevertheless, the non-faradic currents region is not clearly defined as on a polycrystalline Pt electrode in acid medium. It is due to the high capacitance attributed to the electrochemical behavior of IrO_2 and RuO_2. Furthermore, the presence of Pt does not affect the kinetic of OER even though it is a bad catalyst for this reaction. Figure 3 shows the starting potential for OER on RuO_2-Pt and IrO_2-Pt electrodes, 1.3 V and 1.4 V respectively. Finally, the current density registered for the bifunctional electrodes are similar to those registered for the metal oxide electrocatalyst without Ebonex®. This fact suggests a synergic effect between Pt and the metal oxides. Presumably, the mechanism pathway for the oxygen evolution reaction is not affected by the presence of Pt.

3.3. Oxygen evolution activity of the IrO_2 and RuO_2 without and with Pt

The kinetics of the OER on metal oxides based electrodes was studied by recording quasi-stationary lineal voltammetric curves (LV) in a potential range between 1 V and 1.65 V at a scan rate of 5 mV s^{-1} in O_2 – free 0.5 M H_2SO_4 (Data not showed) [27]. Tafel plots were obtained from LV curves for OER before and after ohmic drop (IR_s) correction due to the electrolyte (R_s). This correction was done by subtracting the IR_s to the applied potential (E_{appl}) [28]. R_s-values were evaluated by electrochemical impedance spectroscopy (EIS) for each electrode. R_s values were in the 1.6 Ω – 2.5 Ω interval which are mainly attributed to a combined resistance between the solution resistance and the electrode film resistance.

Figure 4 shows Tafel curves for OER on IrO_2 unsupported electrode before and after IR_s correction. Tafel curves exhibit two linear slopes proving that deviation from linearity observed in the experimental curve is due to ohmic resistance combined with changes in kinetics. For OER on some metal oxides, the first slope is predicted to show a value close to 60 mV dec^{-1} in the low overpotential region (η_{low}) and another higher slope of nearly 120 mV dec^{-1} in the high overpotential region (η_{high}) [6,24].

Table 2 shows kinetics parameters for OER on bifunctional electrodes based on IrO_2, RuO_2 and Pt – nanoparticles. The data were obtained from similar Tafel curves showed in Figure 4. The onset potential values at which the OER occurs is also reported in Table 2.

At low overpotential (η_{low}), Tafel slopes (b) close to 60 mV dec^{-1} were observed for all IrO_2-based and RuO_2-based electrodes. Here, the reaction limiting step (rls) for the oxygen evolution process is attributed to a reorganization of the oxygen-species over the surface. Nevertheless, the Tafel slope data at high overpotential (η_{high}) show values approximately 120 mV dec^{-1}. These results indicate that the rls is the first transfer electron in the electrolysis of the water molecule [9-10,24,28-29]. Tafel slopes values are quite similar to those predicted by the theory. In consequence, the incorporation of platinum does not affect the electrode process for OER. Additionally, the apparently transfer coefficient (α) was obtained from Tafel slopes at high overpotential, Table 2. The a values are close to 0.5 which means that the electron transference is facilitated

by a decrementing of the activation – energy barrier. This fact is influenced by the porosity and roughness degree of the electrode; therefore it shows a highly-electroactive area contrary to a smooth electrode.

The catalytic activity of IrO_2-based and RuO_2-based bifunctional electrodes for OER was evaluated by registering the onset potential (E_{OER}) at which the water decomposition starts and by means of the current density (j) data registered at a specific potential (E =1.5 V(ENH)). E_{OER} and j were extracted from quasi-stationary lineal voltammetric curves after IR-correction. Table 2 shows that the RuO_2 – based electrodes present the lower overpotential (η) versus the thermodynamic potential for OER (1.23 V(ENH)). It is well known that RuO_2 electrocatalyst show a higher activity for OER than IrO_2 [6-8]. The E_{OER}-values showed in Table 2 are in good agreement with those reported in the literature. In addition, RuO_2-Pt/Ebonex electrodes display a higher current density value (j). It is suggested that the RuO_2-Pt mixture presents a synergic phenomena that facilitates the kinetics of oxygen evolution reaction. Additionally, RuO_2 exhibits a major number of active sites due to its high-crystalline degree; as a consequence the O_2-species adsorption/desorption is easier and the electron transference is faster in comparison with those IrO_2-based electrodes. Nevertheless, RuO_2 loses its catalytic activity at highly anodic potential conditions.

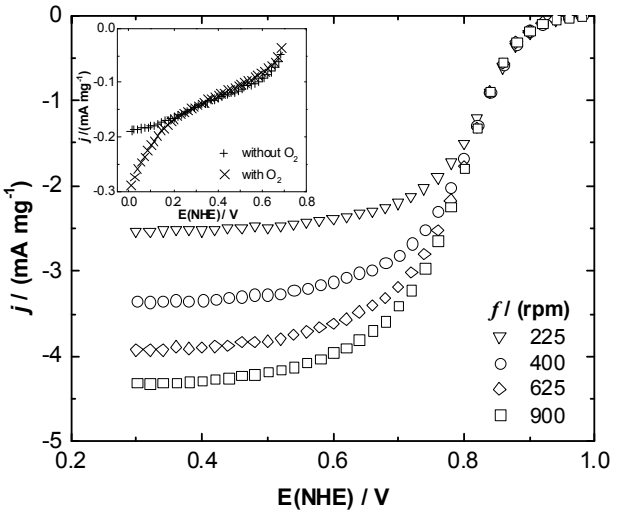

Figure 5. Polarization curves for ORR on (30 wt % IrO_2 – 30 wt % Pt)/Ebonex in O_2-saturated 0.5 M H_2SO_4. Insert: ORR on 30 wt % IrO_2/Ebonex in 0.5 M H_2SO_4without and with O_2 at f =225 rpm. Scan rate = 5 mV s^{-1}. Room Temperature.

3.4. Oxygen reduction activity of the IrO_2 and RuO_2 without and with Pt

The catalytic activity for oxygen reduction of IrO_2 – based and RuO_2 – based electrodes was evaluated by rotating disk electrode (RDE) mesuarements in O_2-saturated 0.5 M H_2SO_4. Figure 5 shows the polarization curves recorded by scanning the potential from the open circuit potential (E_{oc}) to 0.3 V (NHE) at 5 mV s^{-1}. The polarization curves exhibit a cathodic current density beginning around 0.82 V. It means that the mixed IrO_2 – Pt bifunctional electrodes exhibit good catalytic properties for oxygen reduction kinetics.

Figure 5 also shows polarization curves of IrO_2 supported on Ebonex for oxygen reduction (insert) and it is evident that iridum-oxide electrocatalysts do not present intrinsic properties for the kinetic of oxygen reduction. Consequently, the cathodic current density for ORR observed on IrO_2 – Pt electrode is obviously attributed to the incorporation of Pt-nanoparticles. 30wt % RuO_2 – 30 wt % Pt supported on Ebonex® electrodes displayed similar results for ORR than those showed in Figure 5 (Data not showed) [27].

Kinetic parameters for oxygen reduction on IrO_2 – Pt and RuO_2-Pt electrodes were obtained from Tafel plots corrected by mass transfer using the Koutecky – Levich analysis. Duron *et. al.* has reported a fast and simple mathematical methodology to obtain the Tafel slopes by constructing $dE/d(\log j_k)$ vs. E plots [30-31]. $dE/d(\log j_k)$ *vs. E* plots show Tafel slopes values in the –55 mV dec^{-1} to –70 mV dec^{-1} interval at a potential range between 0.97 V to 0.85 V. The Tafel slopes values are in good agreement with the value reported for the ORR on Pt electrode in the low overpotential region which indicates that the reaction limiting step for the oxygen reduction reaction is the oxygen adsorption on the Pt surface previous to the first electron transfer. As a result, it is clear that the metal oxides electrocatalysts do not limit the oxygen reduction reaction.

3.5. Electrochemical impedance spectroscopy performance for OER

EIS measurements for oxygen evolution was carried out on IrO_2 and RuO_2 mixed with Pt unsupported and supported on Ebonex® in O_2-free 0.5 M H_2SO_4 solution in the potensiostatic mode at different anodic potential values with 50 mV increments, using frequen-

Table 2. Onset potential and kinetics parameters for OER on metal-oxides and metal-oxides mixed with Pt –nanoparticles in O_2 – free 0.5 M H_2SO_4.

Surface	E_{OER} (NHE)/V	j /(mA mg^{-1}_{cat}) @ 1.5 V	b / (mV dec^{-1})		α @ b (η_{high})
			η_{low}	η_{high}	
100 wt % IrO_2	1.30	51	61	127	0.47
30 wt % IrO_2*	1.40	42	67	123	0.48
100 wt % RuO_2	1.25	64	55	131	0.45
30 wt % RuO_2*	1.25	43	57	116	0.51
30 wt % IrO_2 – 30 wt % Pt*	1.30	42	65	135	0.44
30 wt % RuO_2 – 30 wt % Pt*	1.25	69	57	105	0.56
100 wt % IrO_2 (Spectrum)	1.40	11	109	-	-

* Supported on Ebonex®.

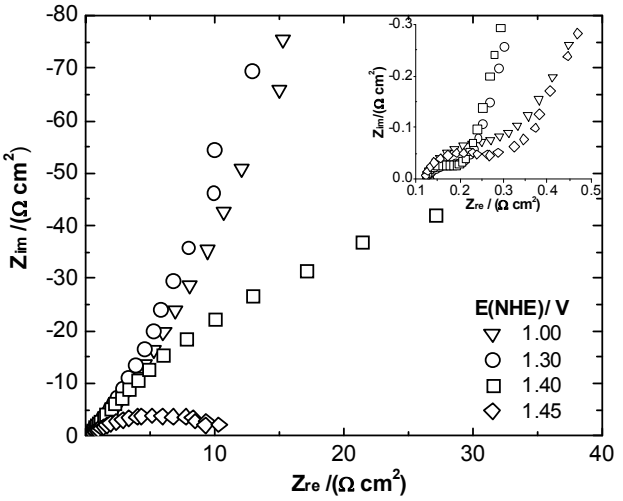

Figure 6. Nyquist plots for OER on IrO_2 – unsupported at different anodic potential values in O_2-free 0.5 M H_2SO_4 solutions. Insert: Nyquist plot zoom at high frequencies.

cies from 100 kHz to 10 mHz and the superimposed perturbation was 10 mV. It was obtained 10 points per decade. Figure 6 shows the Nyquist plots at several anodic potential for OER on IrO_2 unsupported.

According to Figure 6, it is possible to identify the potential value at which the oxygen evolution is taking place. For instance, the Nyquist plot at 1.4 V is revealing that the electron transfer process is beginning. A semi-circle registered at 1.45 V is clearly defined; therefore, this process could be associated to the oxygen evolution reaction. The Nyquist plots recorded at more negative potential values, 1.0 V and 1.3 V, are attributed to mass transference processes, or, probably, to an additional reaction on the metal oxide surface that does not correspond to the oxygen electrode reactions. Actually, our research group is working to get a better interpretation of EIS in order to elucidate the pathway reaction for oxygen evolution on metal oxide and Pt based electrodes.

At high frequencies domain, it is possible to observe the intersection of spectra semi-circles insert in Figure 6. From this point, it was possible to obtain the electrolyte resistance (R_s) value in order to correct the polarization curves for oxygen evolution from ohmic-drop effects (IR_s). In addition, it is observed an additional small semi-loop which is associated to the metal oxide layer.

4. CONCLUSIONS

A systematic study was carried out on the performance of bifunctional electrodes for oxygen reaction based on iridium oxide, ruthenium oxide and Pt electrocatalysts unsupported and supported on Ebonex®. First, the metal oxides were studied without and with the use of Ebonex® as support. The results revealed that there is not a good dispersion of the Ir and Ru oxides on this support. The RuO_2 unsupported and supported shows the best electrocatalytic prorperties for OER. However, it is known that RuO_2 does not have a good electrochemically stability for long-periods at high anodic potentials. On the other hand, IrO_2 electrodes show a higher overpotential to OER, but its long-term stability to corrosion draws itself as the best metal oxide for OER in a URFC. The metal oxides do not show catalytic activity for ORR. Moreover, it was observed that the presence of metal oxides do not influence in the catalytic properties of the Pt for ORR. The incorporation of Pt neither blocks the metal oxide active sites for OER; in contrast, its incorporation allowed reducing the IrO_2 and RuO_2 loads by achieving significantly efficiency – energy gains for water electrolysis. Finally, this work shows the preliminary results for an easy procedure to prepare bifunctional electrodes for the oxygen reactions in URFC. However, more investigations are needed to clarify if exist a bifunctional mechanism between the Pt and IrO_2 for the oxygen evolution process. In addition, it will be interesting to evaluate the kinetic for OER when the Pt load is reduced in the preparation of bifunctional electrodes.

6. ACKNOWLEDGEMENTS

The authors wish to thank the CONACyT FOMIX– Zacatecas (Grant – 81728) and P/PIFI 2007-33-07 for financial support of this work.

REFERENCES

[1] M. Momirlan, T. N. Veziroglu, Int. J. Hydrogen Energy, 30, 795 (2005).
[2] F. Barbir, Solar Energy 78, 661 (2005).
[3] A. Marshall, B. Borresen, G. Hagen, M. Tsypkin, R. Tunold, Energy, 32, 431 (2007).
[4] G. Chen, S. R. Bare, T.E. Mallouk, J. Electrochem. Soc. 149, A1092 (2002).
[5] S.D. Yim, W.Y. Lee, Y.G. Yoon, Y.J. Sohn, G.G. Park, T.H. Yang, Ch. S. Kim, Electrochim. Acta, 50, 713 (2004).
[6] S.Song, H.Zhang, X.Ma, Z.Shao, Int. J. Hydrogen Energy, 33, 4955 (2008).
[7] Y. Zhang, Ch. Wang, N. Wan, Z. Mao, Int. J. Hydrogen Energy, 32, 400 (2007).
[8] L.M. Vračar, N.V. Krstajić, V.R. Radmilović, M.M. Jakšić, J. Electroanal. Chem., 587, 99 (2006).
[9] S. Fierro, T. Nagel, H. Baltruschat, Ch. Comninellis, Electrochem. Comm., 9, 1969 (2007).
[10]L.Ma, S. Sui, Y. Zhai, J. Power Sources 177, 470 (2008).
[11]T. Ioroi, N. Kitazawa, K Yasuda, Y. Yamamoto and H. Takenaka, J. Electrochem. Soc., 147, 2018 (2000).
[12]V. Rashkova, S. Kitova, T. Vitanov, Electochim. Acta., 52, 3794 (2007).
[13]J. Perez, E.R. Gonzalez, E.A. Ticianelli, J. Electrochem Soc., 145, 2307 (1998).
[14]K. Darowicki, J. Orlikowski, J. Electrochem. Soc., 146, 663 (1999).
[15]K.C. Neyerlin, G. Bugosh, R. Forgie, Z. Liu, P. Strassera, J. Electrochem. Soc., 150, 3, E363 (2003).
[16]G. Chen, C.C. Waraksa, H. Cho, D.D. Macdonalk, T.E. Mallouk, J. Electrochem. Soc., 150, 9, E423 (2003).
[17]C. D'Urso, L. Morales, A. Di Blasi, V. Baglio, R. Ornelas, G. Orozco, L.G. Arriaga, V. Antonucci, A.S. Arico, ECS Trans., 11, 1, 191(2007).

[18]J. Kaiser, P. A. Simonov, V. I. Saikovskii, C. Hartnig, L. Jörissen, E.R. Savinova, J. Appl. Electrochem., 37, 1429 (2007).

[19]G.R. Dieckmann, S.H. Langer, Electrochim. Acta, 44, 437 (1998).

[20]S.Y. Park, S.I. Mho, E.O. Chi, Y.u. Kwon, H.L. Park, Thin solid Films, 258, 5 (1998).

[21]J.C. Cruz-Argüelles, M. Sc. Thesis, CIDETEQ S. C. June 2009, Querétaro, México.

[22]A Di Blasi, C. D'Urso, V. Baglio, V. Antonucci, A.S. Aricó, R. Ornelas, F. Mateucci, G. Orozco, D. Beltran, Y. Meas, L.G. Arriaga, J. Appl. Electrochem., 39, 191 (2009).

[23]S.K. Nataraan, J. Hamelin, Electrochim. Acta, 52, 3751 (2007).

[24]M.H.P. Santana, L.A. de Faria, J.F.C. Boodts, J. Appl. Electrochem., 35, 915 (2005).

[25]J. Jirkovský, H. Hoffmannová, M. Klementová, P. Krtila, J. Electrochem. Soc., 153, E111 (2006).

[26]Cyclic voltametry, W. Vielstich in Handbook of Fuell Cell: Fundamentals, Techology and Applicattions, Edited by W. Vielstich, H.A. Gaisteger, A. Lamm. Vol. 2: Electrocatalysis, USA (2003) p. 153.

[27]I.L. Escalante-García, S.M. Durón-Torres, J.C. Cruz y Arriaga-Hurtado L.G., Proceedings of the XXIV meeting of the Mexican Society of Electrochemistry, Paper 105, Puerto Vallarta, Jal, México, May 31 – June 5, 2009.

[28]J.M. Hu J.Q. Zhang, Ch.N. Cao, Int. J. Hydrogen Energy, 29, 791 (2004).

[29]V.V. Kuznetsov, S.A. Chepeleva, M.M. Goldin, V.N. Kudryavtsev, V.N. Fateev, A.G. Volkov, Russian J. of Electrochem. 41, 9, 933 (2005).

[30]C.A. Ramos-Velasco, S.M. Durón-Torres, P.Ibarra-Castro, Proceedings of the XXIII meeting of the Mexican Society of Electrochemistry, Paper 58, Ensenada, B.C., México (2008).

[31]C.A. Ramos-Velasco, M. Galván-Valencia, S.M. Durón-Torres, ECS Trans., 15, 1, 17 (2008).